Thermoelectric, transport, and magnetic properties of the polaron semiconductor $Fe_xCr_{3-x}Se_4$

G. Jeffrey Snyder,* T. Caillat, and J.-P. Fleurial
Jet Propulsion Laboratory/California Institute of Technology, 4800 Oak Grove Drive, MS 277-207, Pasadena, California 91109
(Received 14 January 2000; revised manuscript received 19 May 2000)

The series of compounds $Fe_xCr_{3-x}Se_4$, with $0 \leqslant x \leqslant 3$, has been prepared and various thermoelectric properties measured from 5 to 900 K. Unlike most thermoelectric materials that are band semiconductors with high carrier mobilities, $Fe_xCr_{3-x}Se_4$ are polaronic semiconductors with Hall mobility values, over 100 times smaller. Nevertheless, $Fe_xCr_{3-x}Se_4$ has a surprisingly high thermoelectric figure of merit—within a factor of 5 of state-of-the-art materials. Advantageous as a thermoelectric, $Fe_xCr_{3-x}Se_4$ can be heavily doped both *n*- and *p*-type, switching at $x=0.75$. Although a nearly complete solid solution appears to exist in $Fe_xCr_{3-x}Se_4$, a small but distinct discontinuity was found in the structural and physical properties at $x=1.5$. The electronic transport measurements are consistent with small polaron conductivity, both in the high-temperature activated region, and low-temperature phonon-assisted hopping region proportional to $\exp(-T^{-1/4})$. The magnetic properties are complex and only an approximate phase diagram is given. Only small discontinuities are observed in the transport data at the magnetic transitions. The thermal conductivity of the solid solutions are relatively low, with a glasslike temperature dependence. The thermoelectric figure of merit (ZT) peaks at compositions of $x=0.9$ for *p*-type and about $x=0.5$ for *n*-type. The highest ZT value of 0.15 was found in *p*-type samples at 525 K.

INTRODUCTION

The growth of commercial applications of thermoelectric devices depends primarily on increasing the figure of merit ZT for thermoelectric materials. The figure of merit is defined as $ZT=\alpha^2\sigma T/\lambda$, where α is the Seebeck coefficient, σ the electrical conductivity, λ the thermal conductivity, and T is the absolute temperature. Materials with a large $\alpha^2\sigma$ value, or power factor, are usually heavily doped semiconductors, such as Bi_2Te_3 alloys. For a standard band semiconductor, Z is proportional[1] to $(m^*)^{3/2}\mu/\lambda_L$, where m^* is the carrier effective mass, μ is the carrier mobility, and λ_L is the lattice thermal conductivity. Thus, it is often assumed that the high mobility found in band semiconductors is necessary for a good thermoelectric. Few relatively ionic compounds, where transport proceeds by low mobility polarons, have been considered for thermoelectric applications.[2] For example, various borides and $FeSi_2$ have been studied for high-temperature use. In this paper, $Fe_xCr_{3-x}Se_4$ shows that polaronic semiconductors should be considered for near room-temperature applications even though the carrier mobility is very low.

The thermal conductivity of semiconductors is usually dominated by phonon or lattice thermal conductivity. Thus, another method for finding new, advanced thermoelectric materials is to search for semiconductors with low lattice thermal conductivity.

It is also necessary to find materials that can be readily doped to the optimum carrier concentration for both *p*- and *n*-type materials. New, attractive thermoelectric materials such as filled Skutterudites and Zn_4Sb_3 are often difficult to dope to the optimal *n*- or *p*-type carrier concentration. Therefore, controlling the doping is a major challenge limiting the progress of these materials. An advantage of the $Fe_xCr_{3-x}Se_4$ compounds is their ability to accept a variety of elements over a wide range of compositions, which allows continuous doping from metallic to *n*-or *p*-type semiconductor transport.

Several compounds with the Cr_3S_4 structure type were evaluated for their thermoelectric properties. Of those, Cr_3Se_4 and $FeCr_2Se_4$ were found to be the most promising and representative of the compounds studied.[3] Cr_3Se_4 is a metal with a relatively large Seebeck coefficient, while $FeCr_2Se_4$ is a semiconductor.[4] Furthermore, $FeCr_2Se_4$ has been reported to have room-temperature thermal conductivity of 1.1 mW/cm K, which is an order of magnitude lower than the state-of-the-art thermoelectric material Bi_2Te_3.[5,6] Here we wish to evaluate the solubility limits of Cr and Fe in $Fe_xCr_{3-x}Se_4$, characterize their thermoelectric transport properties, and determine the optimal x for *p*- and *n*-type materials.

The structure of Cr_3S_4 (Fig. 1) consists of hexagonally close-packed S atoms with metal atoms in the octahedral holes as in NiAs. The metal atoms have six anion near neighbors (forming an octahedron) plus two nearby metal atoms along the *c* axis. As suggested by Spitzer[7] the relatively high coordination number of the atoms in this structure may favor low lattice thermal conductivity. Due to the stoichiometry (three metal atoms for every four nonmetal atoms), $\frac{1}{4}$ of the octahedral holes must be vacant. The scattering of phonons by these vacancies should help reduce the lattice thermal conductivity.

In many defect-NiAs compounds, the defects order, increasing the unit cell size and lowering the symmetry (e.g., from hexagonal $P6_3mc$ in NiAs to monoclinic $C2/m$ for Cr_3S_4). The vacancies cut the chains of metal atoms along the NiAs *c* axis into units of three (Fig. 1). Since there are two equivalent end members of the three atom chain for every central atom, one may expect that for the composition AB_2X_4 the *B* atoms would occupy the end positions and the *A* atom the central position of the chain. However, since these two metal atom sites are nearly identical (the central

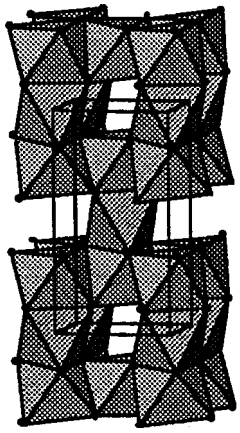

FIG. 1. Illustration of the Cr_3Se_4 unit cell (with Cr_3S_4 structure type) showing Se atoms as small circles and Cr atoms (not shown) at the center of the shaded octahedra. The vertical chain of face sharing octahedra is cut into segments of three units by a vacancy. The monoclinic unit cell is indicated.

site is slightly larger, due to the greater number of vacancies nearby), there can be significant mixing of different atoms on these two sites. Indeed, a full solid solution is found for many of these $A_xB_{3-x}X_4$ compounds.[8]

EXPERIMENT

Polycrystalline samples were prepared by mixing and reacting elemental powders in evacuated silica ampoules for several days at 975–1075 K. The samples were analyzed by x-ray diffractometry to confirm the crystalline structure. The powders were then hot pressed in graphite dies into dense samples, 3 mm long and 12 mm in diameter. The hot pressing was conducted at a pressure of 1400 kg/cm^2 and at 975–1075 K for about 2 h under argon atmosphere. The density of the samples was calculated from the measured weight and dimensions and was found to be greater than 95% of the theoretical density for most samples. Pellets rich in Fe have many cracks and often break apart, making resistivity and thermal conductivity measurements more uncertain for large x.

The samples were also characterized by microprobe analysis which was performed using a JEOL JXA-733 electron superprobe operating at 20 kV and 15 nA. All samples were found to have less than 1% of impurity phases. The elemental concentrations determined from microprobe analysis were within experimental uncertainty (about 1% atomic) of the expected values. The Se concentrations were close to the expected 57% atomic content. Powder x-ray diffraction was used to confirm the Cr_3S_4 structure type, but the monoclinic cell parameters were not refined.

Samples in the form of disks (typically a 1.0-mm-thick, 12-mm-diameter slice) were cut from the cylinders using a diamond saw for electrical and thermal transport property measurements. Temperature dependence of electrical resistivity, Hall effect, Seebeck coefficient, thermal conductivity (by 3ω method), thermal diffusivity, and heat capacity measurements were conducted on selected samples between 2 and 800 K.

A Quantum Design physical property measurement system (PPMS) and indium contacts were used for resistivity measurements below room temperature. Above room temperature Hall effect measurements were performed using a custom designed vacuum furnace and pressure contacts. The four-contact resistivity and Hall effect were measured using the method of van der Pauw.[9] The carrier density was calculated from the Hall coefficient, assuming a scattering factor of 1.0 in a single carrier scheme, by $n=1/R_He$, where n is the density of holes or electrons, and e is the electron charge. The Hall mobility (μ_H) was calculated from the Hall coefficient and the resistivity values by $\mu_H=R_H/\rho$. Normally, the uncertainty is estimated to be $\pm 0.5\%$ and ± 0.2 cm^2/V s for the resistivity and mobility data, respectively. The Hall effect, however, is very small and compounded by the anomalous Hall effect because of the magnetism. Therefore it is difficult to estimate the Hall mobility or carrier concentration. The Hall mobilities calculated in this way for $Fe_xCr_{3-x}Se_4$ were about 0.1 cm^2/V s or less. This equates to carrier concentrations in excess of 10^{20}/cm^3.

The Seebeck coefficient (α) was measured with a high-temperature light pulse technique.[10] The precision of the Seebeck measurement was estimated to be less than $\pm 3\%$. A Quantum Design PPMS was used for low-temperature thermopower and resistivity measurements. Small Au-Fe 7% vs Chromel thermocouples were used to measure both the temperatures and Seebeck voltage across the sample. The Seebeck coefficient is then referenced to copper by subtracting the Seebeck voltage of the thermocouple wires, with respect to copper. The reproducibility of the measurements when thermally cycled is less precise, results in the large relative error reported in Table I, and minor discrepancies between the high- and low-temperature data.

Room-temperature thermal conductivity was measured using the comparison method.[11] High-temperature heat capacity and thermal diffusivity were measured using a flash diffusivity technique.[12] The thermal conductivity (λ) was calculated from the experimental density, heat capacity, and thermal diffusivity values. The overall precision in the thermal conductivity measurements was estimated to be about $\pm 10\%$.

Thermal conductivity was measured on several $Fe_{0.7}Cr_{2.3}Se_4$ samples using the 3ω method.[13] Samples were prepared by polishing, deposition of insulating SiO_2 layer, deposition, and patterning of Au heater-thermometer approximately 75 μm wide and 3 mm long. The excitation and third harmonic was measured by a Quantum Design AC Transport option for the PPMS. The slope of the third harmonic vs log (frequency) was used to calculated the thermal conductivity as described in Ref. 13. Above 50 K, a 200- and 250-mA excitation with frequency between 1 and 40 Hz was used for calculating the slope. At higher frequencies the thermal wavelength decreases, and the thermal conductivity of the dielectric layer begins to contribute. At 100 Hz the thermal wavelength is about 20 μm, similar to the roughness of the samples.

RESULTS AND DISCUSSION

Microprobe results in Table I show an essentially continuous, single phase, solid solubility of Fe_3Se_4 in Cr_3Se_4 allowing for a complete variation in x $(0<x<3)$ in $Fe_xCr_{3-x}Se_4$. This should not be surprising since both compounds have the monoclinic Cr_3Se_4 structure,[14] with different unit cells. The

TABLE I. Results of microprobe analysis and room-temperature thermoelectric properties of the various samples tested. The estimated error of the last digit reported is given in parentheses.

Prepared x	MPA x	Seebeck (μV/K)	Resistivity ($10^{-3}\ \Omega$ cm)	Th. Cond (10^{-3} W/cm K)
0	0	−30(5)	1.2(1)	25
0.25	0.10	−40(5)	1.15(5)	12
0.4	0.36	−50(5)	1.9(1)	15
0.5	0.28	−45(10)	2.6(1)	15
0.5	0.44	−70(15)	3.7(2)	14
0.55	0.50	−80(20)	5.5(1)	14
0.6	0.59	−70(10)	5.0(2)	15
0.64	0.60	−110(20)	20(5)	15
0.68	0.67	−85(10)	13(1)	12
0.7	0.66	−150(20)	70(20)	17
0.72	0.66	−210(20)	250(50)	11
0.75	0.75	150(70)	100(50)	15
0.83	0.82	216(30)	80(20)	13
0.9	0.90	180(10)	19(2)	13
0.97	0.95	115(10)	11(1)	17
1	1.00	110(20)	10(1)	13
1	1.07	190(20)	70(25)	15
1.03	1.03	53(5)	2.7(2)	14
1.1	0.96	120(10)	13(1)	10
1.1	1.11	58(8)	4.5(3)	11
1.5	1.30	10(5)	1.2(2)	14
2	2.07	−5(5)	0.55(5)	
2.5	2.52	−7(2)	6(3)	18
3	3	−12(20)	1.4(4)	34

unit cell parameters of Cr_3Se_4 and Fe_3Se_4 differ sufficiently such that the x-ray diffraction patterns are noticeably distinct. The cell switches abruptly from Cr_3Se_4 type to Fe_3Se_4 type as x increases. It was not clear from the data if a two phase region exists in the transition near $x=1.5$. The magnetic data described below also indicate a discontinuous phase change near $x=1.5$. The primary focus of this study is the metal-semiconductor transition in the Cr rich region $0<x<1.5$.

Electrical resistivity

The $Fe_xCr_{3-x}Se_4$ compounds exhibit a wide variety of electronic properties ranging from metals (resistivity increases with temperature) to *n*- and *p*-type semiconductors. The binary compounds $x=0$ and $x=3$ are metals having room-temperature resistivity (ρ) of about 10^{-4}–$10^{-3}\ \Omega$ cm, while near $x=1$ the materials are semiconducting.

For samples with $x \geqslant 0.4$ the resistivity decreases with temperature, like for a semiconductor. The high-temperature electrical resistivity for various x is shown in Fig. 2. Near room temperature, these samples behave like extrinsic semiconductors, or small polaron conductors. The resistivity due to small polaron hopping conduction has only a slightly different temperature dependence $[T\exp(E_a/kT)]$ than that expected of a semiconductor $[\mu^{-1}\exp(E_a/kT)]$ where the mobility μ is proportional to $T^{-3/2}$ for many semiconductors.

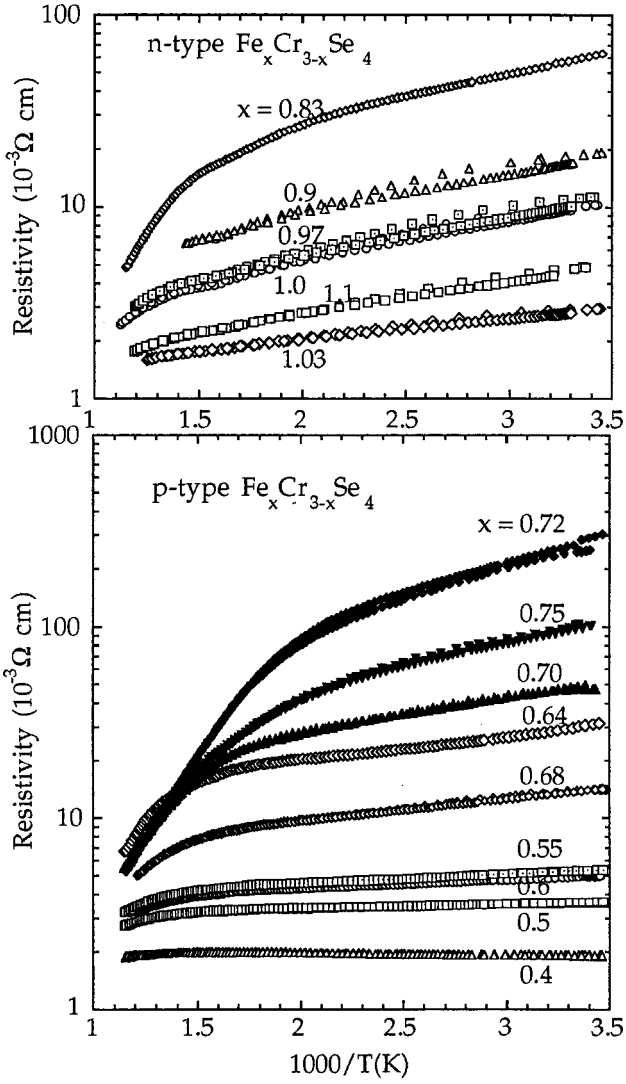

FIG. 2. High-temperature electrical resistivity of $Fe_xCr_{3-x}Se_4$. Heating and cooling curves are shown. Open symbols are *p*-type samples and closed symbols are *n*-type.

Both forms are dominated by an exponential with characteristic energy E_a. For the materials described here the resistivity data are not sufficiently well described by either of the exact forms to determine the transport mechanism.

Nevertheless, band semiconductor transport characteristically has carriers with high mobility and low concentration. Small polarons typically have high concentration and low mobility on the order of 0.1 $cm^2/V\ s$,[15] consistent with measurements of $Fe_xCr_{3-x}Se_4$.

In the *p*-type samples, $x \approx 0.9$, the resistivity activation energy near room temperature is about 0.04 eV while the *n*-type materials have lower extrinsic activation energies (about 0.02 eV). These values presumably reflect the polaron hopping barrier energy or the energy required to excite carriers from acceptor or donor levels.

In the highest resistance samples $0.72<x<0.83$ there is an intrinsic regime at high temperature. Here the measured resistivities approach a common curve. From the slope of this high-temperature/high-resistance regime, we calculate an activation energy of (4000 K) 0.34 eV. A semiconducting band gap of 0.68 eV would give such an activation energy;

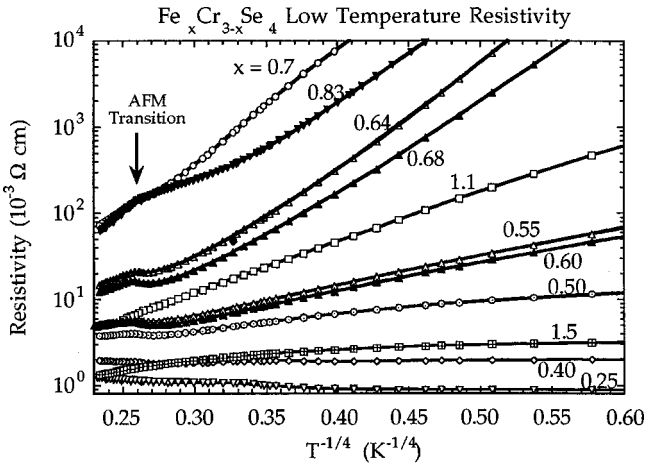

FIG. 3. Low-temperature electrical resistivity of $Fe_xCr_{3-x}Se_4$. Showing the consistency with phonon assisted hopping $\exp(T^{-1/4})$ temperature dependence and the antiferromagnetic transition at 210 K. The change in slope due to the ferromagnetic transition at lower temperature is less noticeable.

however, such a large gap is unlikely to exist in a calculated band structure since partially filled *d* bands are expected.[3]

A close inspection of the resistivity as a function of temperature reveals small nonlinearities and hysteresis. This may be due to magnetic or structural changes, or even loss of Se at high temperatures. For example, in the high-temperature resistivity data for samples with $0.2<x<1.4$ a reversible discontinuity is found at about 620 K. This is likely due to a structural phase transition at this temperature. The transition temperature increases as the Fe content increases; from 600 K for $x\approx0.25$ to 650 K for $x\approx1.35$.

There is also a discontinuity in the low-temperature resistivity ($x<1.5$, and more pronounced for smaller x) at about 210 K (Fig. 3) which is due to the antiferromagnetic transition (see below).

The low-temperature resistivity of the semiconducting samples rises slower than $\exp(1/T)$ as T decreases. The data closely correspond to $\exp(1/T^{1/4})$ (Fig. 3), which is expected for phonon assisted hopping of small polarons[16] (as well as variable range hopping). The phonon-assisted hopping mechanism is expected to dominate at temperatures less than half the Debye temperature.

Thermopower

The room-temperature thermopower of the chromium-rich compounds tend to be negative (Table I). The Seebeck coefficient of these metals ($x<0.4$) is linear (Fig. 4) with temperature T as expected from the diffusion thermopower. For an electron gas the diffusion thermopower is given by[17]

$$\frac{\pi^2 k_B^2 T}{3e}\left(\frac{\partial \ln[\sigma(E)]}{\partial E}\right)_{E_F}.$$

The linear extrapolation of the thermopower to a nonzero value (Fig. 5) may be due to the phonon drag component to the thermopower.[18]

The semiconducting compositions have a larger thermopower that reaches an absolute maximum as is expected for semiconductors. The *p*-type compositions (Fig. 6) reach a

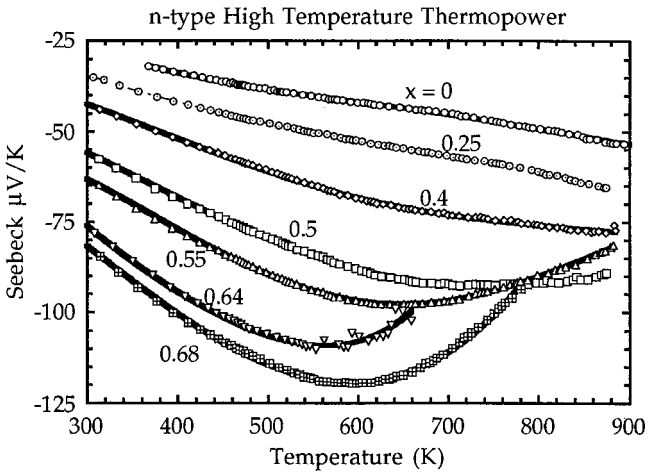

FIG. 4. High-temperature thermopower of *n*-type $Fe_xCr_{3-x}Se_4$.

maximum Seebeck coefficient at about 450 K. At higher temperatures, the thermopower begins to follow the shape of a common $1/T$ law expected for small polaron semiconductors[15,19] where the width of the polaronic bands is much less than kT. The *n*-type compositions (Fig. 7) have a lower absolute thermopower, which peaks at a higher temperature, about 600 K or more.

Metal-semiconductor transition

In order to better understand the variation in the transport properties as x changes, the room temperature values for the resistivity and Seebeck coefficient are analyzed. Although the thermoelectric properties are not optimal at room temperature, this is a convenient and representative temperature.

The transport behavior at room temperature qualitatively follows that expected from a doped semiconductor. The room-temperature resistivity peaks (exponentially) near $x=0.75$ (Fig. 8). The thermopower also rises and then changes sign at the same composition (Fig. 9). This is classic behavior of a semiconductor being doped from *n*-type to *p*-type. A classic semiconductor however, does not require such a large variation in concentration to make a noticeable change in the properties.

The semiconducting nature of $x=1$ might be expected for $Fe^{2+}Cr_2^{3+}Se_4$. The Cr is expected to be d^3 and strongly ex-

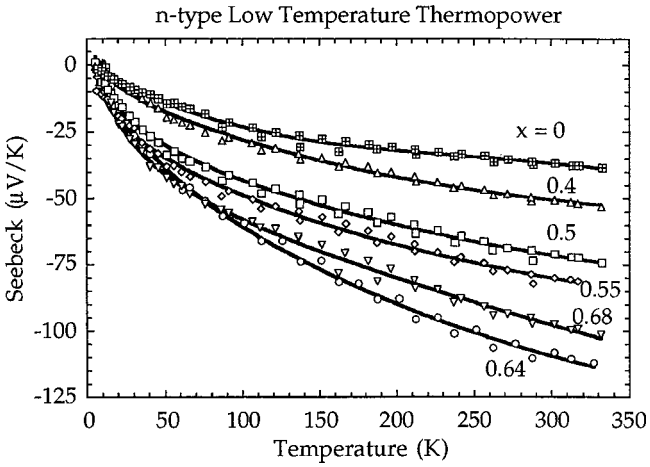

FIG. 5. Low-temperature thermopower of *n*-type $Fe_xCr_{3-x}Se_4$.

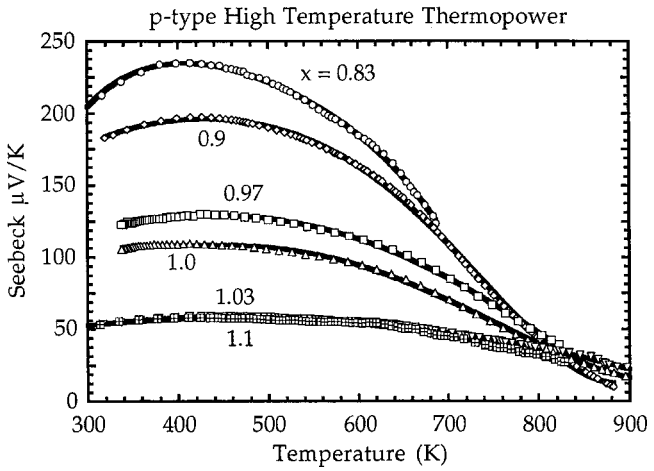

FIG. 6. High-temperature thermopower of *p*-type $Fe_xCr_{3-x}Se_4$.

change split so that the majority spin t_{2g} band is completely filled. The Fe may be low spin d^6 ($S=0$) also having a completely filled t_{2g} band. With such an electron configuration, one would expect $FeCr_2Se_4$ to be a small band gap semiconductor with the gap between different metal *d* bands.

Such a simplified picture is inconsistent with other experimental results. Low spin Fe^{2+} is unlikely and inconsistent with the large Curie-Weiss paramagnetic moment (see below). High spin Fe^{2+} will have partially filled *d* levels to produce metallic bands. Furthermore, this simple electron counting would imply that the most semiconducting composition would have $x=1$. The replacement of Fe^{2+} with Cr^{3+} should add holes making the sample *p*-type and more conductive while replacement of Cr^{3+} with Fe^{2+} will produce *n*-type conduction. The data clearly show such a transition from *n*-type to *p*-type (Fig. 9) with a corresponding maximum in the electrical resistivity (Fig. 8) not at $x=1$ but near $x=0.75$.

It is unlikely that a more complex band calculation will explain the semiconducting nature of the $x=0.75$ compound unless electron localization is considered. $Fe_xCr_{3-x}Se_4$ will probably have complex band structures with many metal *d* bands near the Fermi level. If these electrons are localized on the metal atoms, which are relatively distant from one another, electron conduction may not be metallic but proceed

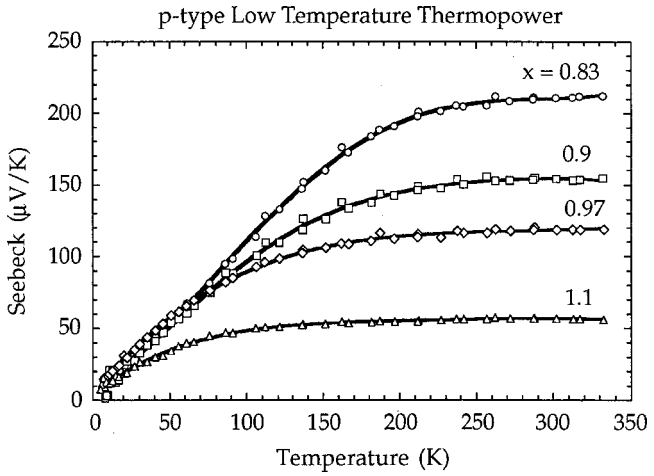

FIG. 7. Low-temperature thermopower of *p*-type $Fe_xCr_{3-x}Se_4$.

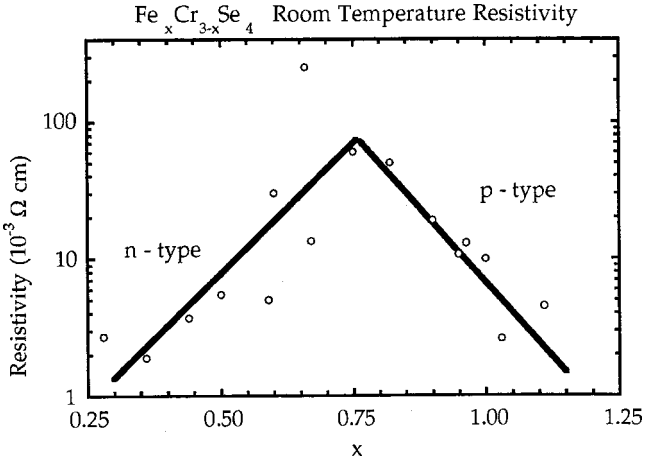

FIG. 8. Room-temperature electrical resistivity of $Fe_xCr_{3-x}Se_4$ shows maximum resistivity near $x=0.75$.

by a (small polaron) hopping mechanism. Such a compound may also be considered a Mott insulator.

Magnetism

The $Fe_xCr_{3-x}Se_4$ system exhibits a variety of different and complex magnetic phenomena. Many of the results can be summarized in the magnetic phase diagram of Fig. 10. For $x \leqslant 1.5$, $Fe_xCr_{3-x}Se_4$ shows an antiferromagnetic transition in the susceptibility below 225 K. Then at a lower temperature (about 75 K) the sample becomes ferromagnetic, or more precisely, ferrimagnetic.

Such a sequence of transition can be seen in Fig. 11 for $x=1$. Above 220 K the magnetic susceptibility χ follows the Curie-Weiss formula $\chi_{\mathrm{mol}}=(N_A\mu_B^2/3k_B)\ p^2/(T-\Theta)$, where *p* is the effective magnetic moment. The data fit well with $p^2=62\mu_B^2$/formula, and $\Theta=-575$ K. The latter indicates strong antiferromagnetic interactions before the antiferromagnetic transition at the Néel temperature $T_N=220$ K. The measured effective moment is somewhat larger than that expected ($p^2=54$) for high spin Fe^{2+} ($d^6, S=2$) and Cr^{3+} ($d^3, S=\frac{3}{2}$). This may indicate the presence of some high spin

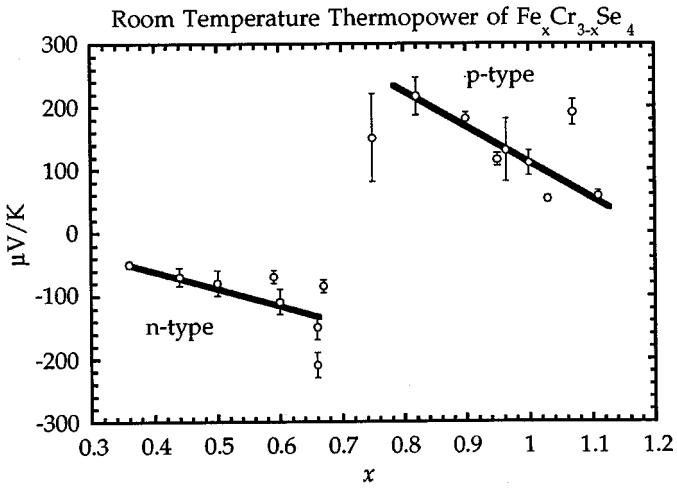

FIG. 9. Room-temperature thermopower of $Fe_xCr_{3-x}Se_4$ shows *n*-type doping for $x<0.75$ and *p*-type behavior for $x>0.75$.

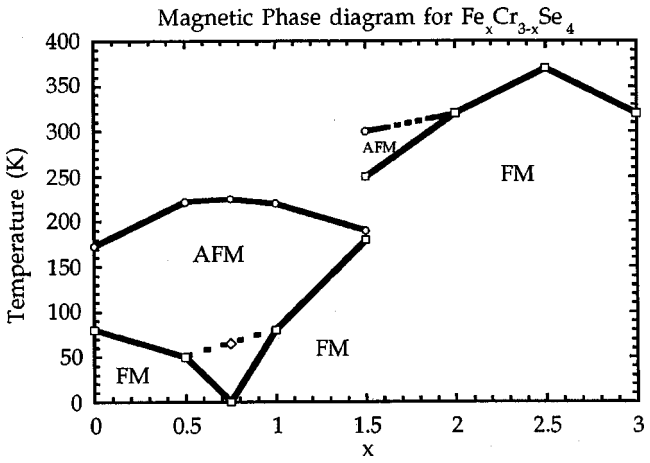

FIG. 10. Magnetic phase diagram of $Fe_xCr_{3-x}Se_4$. AFM denotes regions of antiferromagnetism while FM denotes ferrimagnetism or ferromagnetism. Data are from this work and Refs. 20 and 21.

Cr^{2+} $(d^4, S=2)$ and Fe^{3+} $(d^5, S=\frac{5}{2})$. A sample of $Fe^{3+}Cr^{2+}Cr^{3+}Se_4$ would have $p^2=74$.

At low temperature the $x=1$ sample has a small ferromagnetic component. At 5 K the net ferromagnetic moment is only $0.007\mu_B$ from the extrapolation of the 5-K hysteresis loop to zero field. The 2000 G susceptibility curve shows a ferromagnetic magnetization curve with a Curie temperature of 80 K. The field cooled remnant magnetization (measured in zero applied field) decreases rapidly as the temperature is increased, due to the decreasing coercive field (about 250 G at 5 K). At the Curie temperature this remnant moment vanishes. However, before vanishing, the net remnant moment becomes zero at about 45 K and then negative up to the Curie temperature. In zero applied field, this must be due to ferrimagnetism and not any ferromagnetic impurities. In ferrimagnetism, the various magnetic sublattices oppose each other but do not exactly cancel, resulting in a small, but nonzero net magnetic moment. However, the temperature dependence of the magnetic moment in each sublattice may be different which can lead to the weaker sublattice becoming stronger. The reversal of the net magnetic moment occurs at the compensation temperature (45 K).

The parent compound Cr_3Se_4 is known to have a complex magnetic structure with magnetic transitions at 80 and 173 K

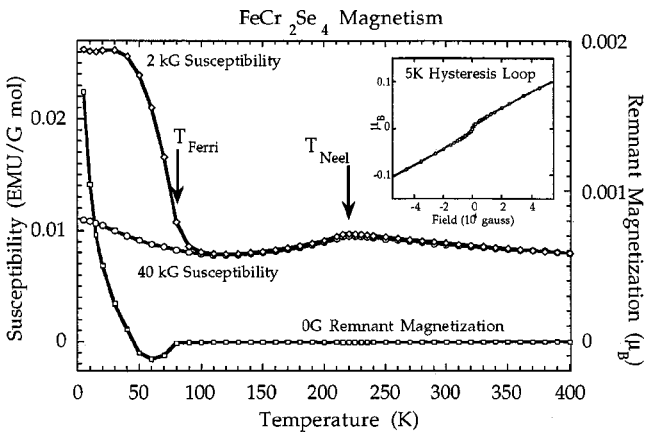

FIG. 11. Magnetic properties of $FeCr_2Se_4$.

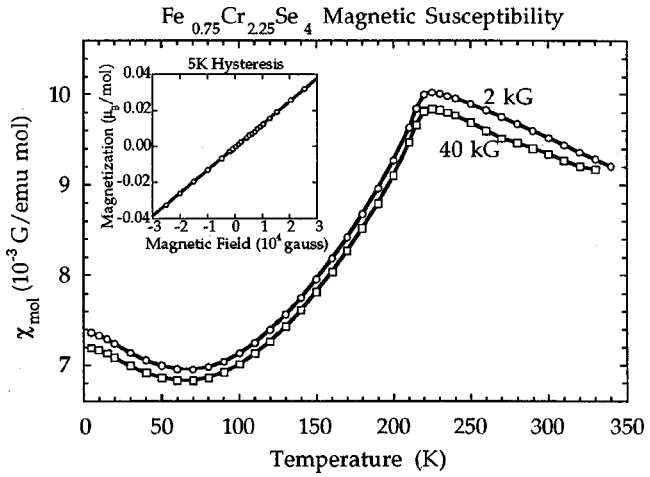

FIG. 12. Magnetic properties of $Fe_{0.75}Cr_{2.25}Se_4$.

(see Ref. 21 for recent discussion). The exact magnetic structure of $Fe_xCr_{3-x}Se_4$ is certainly also quite complex. Variations in the magnetic properties have been found to depend on the Se concentration.[22,23] It is expected that $Fe_xCr_{3-x}Se_4$ will be similarly affected by Se nonstoichiometry as well as Fe concentration.

For the $x=0.5$ sample, the data are qualitative similar, with larger net ferromagnetic moment and lower ferrimagnetic transition temperature.

However, for the $x=0.75$ sample, the most insulating composition, the ferromagnetism appears to be suppressed. There is no nonlinearity in the 5-K hysteresis, and no dramatic increase in the susceptibility (Fig. 12). There exists only a shallow minimum in the susceptibility at the temperature one might expect to see a ferromagnetic transition (65 K).

Near $x=1.5$ there appears to be a discontinuous change in the magnetic properties to those similar to the other end member Fe_3Se_4.[24] The iron rich samples $(x>1.5)$ show a direct transition to a ferrimagnetic phase above 300 K, as demonstrated in Fig. 13 for $x=2$. The coercive field for these materials is much larger, over 10 k gauss. Because of this large field, when the sample is cooled in 2 k gauss, the resulting magnetization is negative at low temperature. During cooling the sample is magnetized with the high-temperature

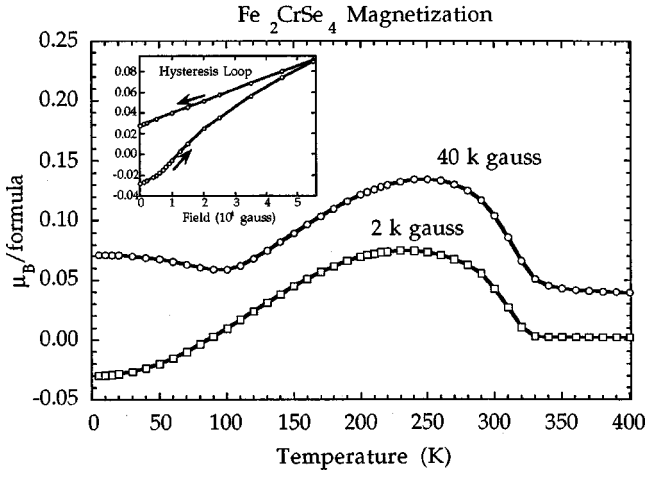

FIG. 13. Magnetic properties of Fe_2CrSe_4.

dominant sublattice pointing in the positive direction. Below the compensation temperature (near 75 K) the net magnetization reverses. However, the 2 k gauss field is too small to reorient the magnetization, so the measured magnetization is negative. In higher fields (e.g., 40 k gauss data), greater than the coercive field, the magnetization is always positive, with a local minimum near the compensation temperature. Only in the $x=1.5$ sample, which may have two magnetic phases present, was there a weak indication of antiferromagnetism before the onset of ferromagnetism.

The various magnetic transitions have little impact on the thermoelectric properties. The antiferromagnetic transition produces a small but noticeable cusp in the resistivity for the Cr-rich samples as can be seen in Fig. 3. However, there is no significant change in the Seebeck coefficient (Fig. 5). The onset of magnetic ordering should decrease the extent of magnetic scattering and possibly increase the mobility of the charge carriers; however the effect on the thermoelectric properties is minimal. Since the internal magnetic structure does not greatly influence the thermoelectric properties, an external magnetic field will probably also insignificantly alter the thermoelectric properties.

Thermal conductivity

The thermal conductivity λ is given by the sum of the electronic λ_E and lattice contributions λ_L. λ_E is directly related to the electronic conductivity: $\lambda_E = L\sigma T$, where L is the Lorenz factor. The Lorenz factor typical for metals (2.4×10^{-8} J^2/K^2 C^2) is used to calculate the electronic contribution, although a smaller Lorentz factor may be more appropriate for these materials.[3]

Most of the $Fe_xCr_{3-x}Se_4$ compounds studied have room temperature thermal conductivity (Table I) of $14\pm4\times10^{-3}$ W/cm K with no noticeable composition dependence for the ternary compounds. The binary compounds ($x=0,3$) are expected to have a larger lattice contribution due to the lack of alloy scattering. The extremely low thermal conductivity values ($\approx1\times10^{-3}$ W/cm K) reported in the literature for Fe_2CrSe_4 (Ref. 25) and $FeCr_2Se_4$ (Refs. 5 and 6) were not observed.

The thermal conductivity measured by the 3ω method is shown in Fig. 14. The sample measured, $x=0.7$, has a low carrier concentration, so that the thermal conductivity is dominated by the lattice contribution. The lattice thermal conductivity measured, presumed to be representative for x in the region of interest ($0.4<x<1.5$), shows a very flat temperature dependence above the antiferromagnetic transition temperature 220 K (barely noticeable in the data) to well above room temperature (700 K from thermal diffusivity of $x=0.97$ sample). This is characteristic of complex structures such as glasses, and probably due to the disordered nature of the ionic and perhaps magnetic structure. Below the Néel temperature, the thermal conductivity behaves more like common crystalline solid solutions that have large lattice thermal conductivity that is proportional to $1/T$.[26]

Thermoelectric properties

Since the thermal conductivity for the $Fe_xCr_{3-x}Se_4$ compounds are very close and change little with temperature, the controlling factor to the thermoelectric figure of merit is the power factor ($\alpha^2\sigma$). Figure 15 shows that the various samples measured cover a wide range of resistivity and Seebeck coefficient values. The trend toward higher thermopower in samples with high resistance is typical but the slope is about half that of a conventional semiconductor with low carrier concentration. Using classical statistics, appropriate at low carrier concentration, this slope is $\partial\alpha/\partial\ln(\sigma)=k/e$ which leads to a 200-μV/K change per decade of resistivity.[27] Considering this relationship and the trend shown in Fig. 15, we can be confident that nearly optimal samples have been measured. Therefore, we conclude that the maximum power factor at room temperature for $Fe_xCr_{3-x}Se_4$ is about 1–1.5 μW/cm K^2.

The thermoelectric figure of merit ZT has been calculated for the optimal p-type composition, $x=0.9$. A maximum ZT of about 0.15 is found at 525 K (Fig. 16). This is about a factor of 6 smaller than state-of-the-art materials. Considering the low carrier mobilities of $Fe_xCr_{3-x}Se_4$, this is a surprisingly high number. Typical thermoelectric materials have

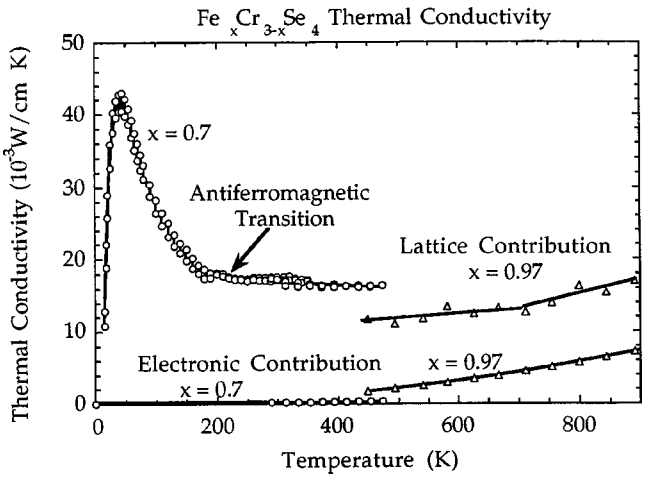

FIG. 14. Thermal conductivity of $Fe_xCr_{3-x}Se_4$. The 3ω results for $x=0.7$ (due to lattice) show a flattening at the antiferromagnetic transition. The lattice contribution for $x=0.97$, from thermal diffusivity data, follows a similar trend to higher temperatures.

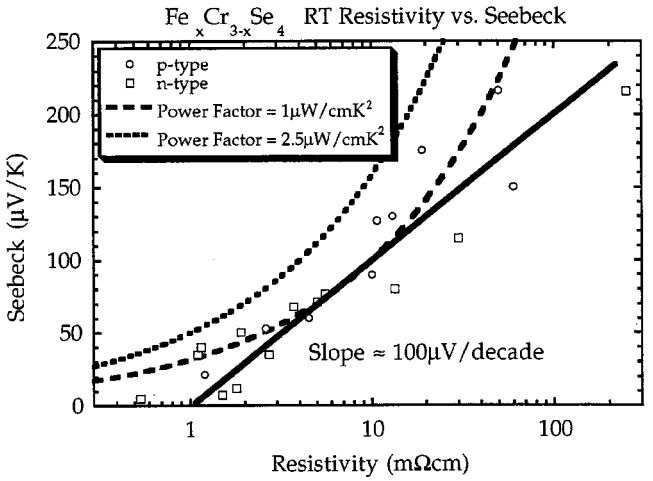

FIG. 15. Room-temperature (RT) Seebeck vs resistivity values for various x in $Fe_xCr_{3-x}Se_4$. The trend in the data shows that the maximum RT power factor that can be expected from optimal doping is about 1 μ W/cm K^2.

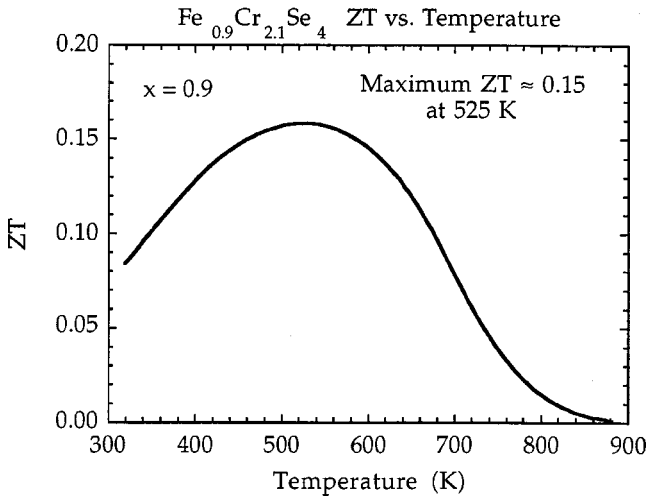

FIG. 16. *ZT* as a function of temperature for the optimal *p*-type composition $Fe_{0.9}Cr_{2.1}Se_4$.

carrier mobilities greater than 10 $cm^2/V\,s$, whereas $Fe_xCr_{3-x}Se_4$ have mobilities about 100 times less. This is due to the hopping method of transport, the increased electron scattering from the transition metal magnetic moments (magnon scattering) and perhaps due to the lower covalency of these materials as compared to conventional thermoelectric semiconductors. The same narrow bands that lead to the localization of the charge carriers, should also produce large effective masses $(m^*/m \sim 4)$, enhancing the thermopower. The large thermopower enhanced by the large effective mass, is then offset by the high resistivity because of the low mobility.[28]

SUMMARY

Traditional thermoelectric materials are band semiconductors. In our search for new thermoelectric materials, we have chosen to study $Fe_xCr_{3-x}Se_4$, which is a polaronic semiconductor. Despite the fact that polaron semiconductors have very low mobilities, over 100 times smaller than conventional thermoelectric materials, $Fe_xCr_{3-x}Se_4$ has a surprisingly high thermoelectric figure of merit—within a factor of 5 of state-of-the-art materials. The low mobility is apparently offset by the large effective mass, enhancing the thermopower.

An advantage of the $Fe_xCr_{3-x}Se_4$ compounds is the chemical versatility of the structure, allowing continuous doping from metal to *n*- and *p*-type semiconductors. Optimization of the carrier concentration is one of the many challenges for finding new thermoelectric materials.

Although a nearly complete solid solution appears to exist in $Fe_xCr_{3-x}Se_4$, a small but distinct discontinuity was found in the structural and physical properties at $x=1.5$. The metal-semiconductor transition occurs in the Cr-rich region centered around $x=0.75$. The resistivity and magnitude of the Seebeck coefficient maximizes at this comparison while the thermopower changes from *n*-type to *p*-type. Such a behavior is a classic example of a doped semiconductor and ideal for thermoelectric applications. However the location of the transition at $x=0.75$ is unexpected and has not been explained.

The electronic transport measurements are consistent with small polaron conductivity. At high temperatures the Hall mobility is very low with a thermally activated conductivity. At low temperatures, phonon-assisted hopping is observed.

The magnetic properties are complex but do not affect the thermoelectric properties significantly. Only minor discontinuities are observed in the transport data at the magnetic transitions.

The thermal conductivity of the solid solutions are relatively low, with a glasslike temperature dependence, particularly above the Néel temperature, presumably due to the complex, disordered crystal structure.

The thermoelectric figure of merit (*ZT*) maximizes at compositions of $x=0.9$ for *p*-type and about $x=0.5$ for *n*-type. The highest *ZT* of 0.15 was found in *p*-type samples at 525 K.

ACKNOWLEDGMENTS

We would like to thank Josh Maurer, A. Zoltan, L. D. Zoltan, S. Chung, and A. Borshchevsky for their help on this project. This work was carried out at the Jet Propulsion Laboratory—California Institute of Technology, under contract with NASA and supported by the U.S. Defense Advanced Research Projects Agency, Grant No.E407.

*Email address: jeff.snyder@jpl.nasa.gov

[1] A. F. Ioffe, *Semiconductor Thermoelements and Thermoelectric Cooling* (Infosearch Limited, London, 1957).

[2] V. K. Zaitsev, S. A. Ktitorov, and M. I. Fedorov, in *Thermoelectric Handbook*, edited by M. Rowe (CRC, Boca Raton, 1995), p. 311.

[3] G. J. Snyder, T. Caillat, and J.-P. Fleurial, in *Thermoelectric Materials 1998—Next Generation Materials for Small-Scale Refrigeration and Power Generation Applications*, edited by T. M. Tritt, M. G. Kanatzidis, G. D. Mahan, and H. B. Lyon, Jr. Mater. Res. Soc. Symp. Proc. No. 545 (Materials Research Society, Warrendale, PA, 1999), Vol. 545, p. 333.

[4] L. M. Valiev, I. G. Kerimov, S. K. Babaev, and Z. M. Namazov, Inorg. Mater. **11**, 176 (1975).

[5] V. A. Ivanova, D. S. Abdinov, and G. M. Aliev, Phys. Status Solidi **24**, K23 (1967).

[6] G. B. Abdullaev, G. M. Aliev, V. A. Ivanova, and D. S. Abdinov, Heat Transfer-Sov. Res. **5**, 30 (1973).

[7] D. P. Spitzer, J. Phys. Chem. Solids **31**, 19 (1970).

[8] *Semiconductors*, edited by O. Madelung and M. Schulz, Landolt-Börnstein, New Series, Group III, Vol. 17, Pt. h (Springer-Verlag, Berlin, 1987); *Magnetic and other Properties of Oxides and Related Compounds*, edited by K.-H. Hellwege and A. M. Hellwege, Landolt-Börnstein, New Series, Group III, Vol. 12, Pt. b (Springer-Verlag Berlin, 1970); *Magnetic and other Properties of Oxides and Related Compounds*, edited by K.-H. Hellwege and A. M. Hellwege, Landolt-Börnstein, New Series, Group III, Vol. 4, Pt. b (Springer-Verlag, Berlin, 1978).

[9] L. J. van der Pauw, Philips Res. Rep. **13**, 1 (1958).

[10] C. Wood, L. D. Zoltan, and G. Stapfer, Rev. Sci. Instrum. **56**, 719 (1985).

[11] D. M. Rowe, *Thermoelectric Handbook* (Ref. 2).

[12] J. W. Vandersande, C. Wood, A. Zoltan, and D. Whittenberger, in *Thermal Conductivity* (Plenum, New York, 1988), p. 445.
[13] D. G. Cahill, Rev. Sci. Instrum. **61**, 802 (1990).
[14] R. W. G. Wyckoff, *Crystal Structures* (Interscience, New York, 1963).
[15] D. Emin, in *Electronic and Structural Properties of Amorphous Semiconductors*, edited by P. G. LeComber (Academic, London 1973).
[16] A. Moliton and B. Lucas, Ann. Phys. (Paris) **19**, 299 (1994).
[17] R. D. Barnard, *Thermoelectricity in Metals and Alloys* (Wiley, New York, 1972).
[18] H. J. Trodahl, Phys. Rev. B **51**, 6175 (1995).
[19] M. Jaime, M. B. Salamon, M. Rubinstein, R. E. Treece, J. S. Horwitz, and D. B. Chrisey, Phys. Rev. B **54**, 11 914 (1996).
[20] D. A. Guseinov, M. A. Aldzhanov, R. Z. Sadykhov, and N. G. Guseinov, Inorg. Mater. (Transl. of Neorg. Mater.) **25**, 1018 (1989).
[21] S. Ohta and Y. Adachi, J. Magn. Magn. Mater. **164**, 225 (1996).
[22] A. Maurer and G. Collin, J. Solid State Chem. **34**, 23 (1980).
[23] M. Yuzuri, J. Phys. Soc. Jpn. **35**, 1252 (1973).
[24] N. G. Aliev, N. G. Guseinov, I. G. Kerimov, R. Z. Sadykhov, and D. A. Guseinov, Inorg. Mater. **13**, 633 (1977).
[25] N. R. Akhmedov, N. Z. Dzhalilov, G. M. Aliev, and D. S. Abdinov, Inorg. Mater. **10**, 711 (1974).
[26] C. M. Bhandari and D. M. Rowe, *Thermal Conduction in Semiconductors* (Wiley Eastern Limited, New Delhi, 1988).
[27] D. M. Rowe and C. M. Bhandari, *Modern Thermoelectrics* (Reston, Reston, VA, 1983), p. 25.
[28] R. R. Heikes and R. W. Ure, *Thermoelectricity: Science and Engineering* (Interscience, New York, 1961), p. 344.